# Influence of the technique for producing lithium-titanium ferrite ceramics on its electrical properties

**A P Surzhikov, A V Malyshev and S A Lamonova**

National Research Tomsk Polytechnic University, Tomsk, Russia

E-mail: malyshev@tpu.ru

**Abstract.** The patterns of electrical, dielectric, magnetic, and structural characteristics for the lithium-titanium ferrite ceramics, prepared in different technological conditions have been investigated for the first time. The determining factor of the obtained patterns is structural redistribution of iron ions over the sublattices and their diffusion from the grain boundary in the volume of the ferrite ceramics grain.

**Keywords:** Ferrite; Dielectric permittivity; Saturation magnetization.

## 1. Introduction

Modern development and updating of electronic equipment specifies increasingly strict requirements to the properties of ferrite materials. Lithium ferrites attract considerable attention of researchers due to feasibility of their application in microwave technology as circulators, isolators, and phase shifters due to high resistivity, low eddy current and fairly low cost.

It is well-known [1] that electrical properties of ferrite ceramics are sensitive to its composition and microstructure, which in turn are determined by technological conditions of sintering. Changes in temperature and sintering time cause redistribution of iron cations over the octahedral and tetrahedral sites in the spinel lattice. Therefore, the study of the interrelation between the conditions of ferrite ceramics sintering with its main physical characteristics is of current interest.

## 2. Experimental techniques

The studied samples were sintered under different conditions: sintering temperature $T_s$ = 1283 K and 1373 K; sintering time $t_s$ = 2, 4, and 7 hours. The technology of sample preparation was similar to that described in [2]. The sintering conditions were close to those currently used for production of 3SCH-18 ferrite.

The dielectric parameters of ferrite were obtained with a measurement setup based on automatic meter LCR-819 Goodwill, a special measuring cell and Origin to process the experimental results [3].

The saturation magnetization of the ferrite was measured at room temperature in pulsed magnetic fields with a maximum strength of 5 kOe using an original magnetometer [10].

The structural parameters of powder samples were studied with the X-ray diffractometer X'TRA.

## 3. Result and discussion

Figure 1 presents the experimental temperature dependence of the complex permittivity components. As can be seen in the Figure, increase in the values of the dielectric permittivity occurs at least within two stages. As the temperature grows, the slope of the curve increases, which implies the involvment of the second type of relaxators of higher concentration.

To approximate the experimental curves and to obtain the values of the dielectric parameters we used both the classical expression for the Debye relaxation polarization (1–4) and the expressions for the Wagner-Koops mechanism of interlayer polarization [8]. These models are most frequently used for mathematical processing of the measurement results obtained for dielectric ferrite ceramics [6, 7, 11].

The expressions for the complex permittivity components ε′ and ε″ of the classical Debye model for two types of dipoles [7] are as follows:

$$\varepsilon' = \varepsilon_\infty + \frac{\varepsilon_2 - \varepsilon_\infty}{1+(\omega\cdot\tau_1)^2} + \frac{\varepsilon_{sf} - \varepsilon_2}{1+(\omega\cdot\tau_2)^2} \quad (1)$$

$$\varepsilon'' = \frac{(\varepsilon_2 - \varepsilon_\infty)\cdot\omega\cdot\tau_1}{1+(\omega\cdot\tau_1)^2} + \frac{(\varepsilon_{sf} - \varepsilon_2)\cdot\omega\cdot\tau_2}{1+(\omega\cdot\tau_2)^2} + \frac{\sigma_a}{\varepsilon_0\cdot\omega} \quad (2)$$

In these expressions, $\varepsilon_\infty$ is the dielectric permittivity due to inertialess polarization; $\varepsilon_{sf}$ is static effective dielectric permittivity; $\tau_1=\tau_{01}\cdot\exp[E_{a1}/(k\cdot T)]$ is the expression for the characteristic time of relaxation polarization for dipoles of the first type; $E_{a1}$ and $\tau_{01}$ are the activation energy of relaxation for relaxation oscillators of the first type and the pre-exponential factor, respectively; $\tau_2$ is the characteristic time of relaxation polarization for dipoles of the second type, $\varepsilon_0$ is vacuum permeability.

$\sigma_a = \sigma_{0a}\cdot\exp[-E_{a\sigma}/(k\cdot T)]$ and $E_{a\sigma}$ are the conductivity and the activation energy of the alternating current electrotransport; k is the Boltzmann constant; $\varepsilon_2$ is the dielectric constant in the absence of the relaxation oscillators of the second type; ω is angular frequency.

Classical expressions (1, 2) used for calculations did not allow satisfactory approximation of the experimental temperature dependence for ε′ and ε″ components. Similar results were obtained in calculations when using the expressions for the Wagner-Koops polarization model [8, 9].

However, frequency-decreasing expressions (3, 4) used for $\tau_{0f}$ and $\varepsilon_{sf}$ parameters in (1, 2)

$$\tau_{0f}=A\cdot\omega^{-q1} \quad (3)$$

$$\varepsilon_{sf}=B\cdot\omega^{-q2} \quad (4)$$

provide satisfactory approximation of the temperature dependence for ε′ and ε″ components for two types of relaxation oscillators (Fig. 1). Symbols are the experimental data and lines are the calculated curves (the dependences for two of the six samples). Mathematical processing implied automatic adjustment of the parameters in expressions (1–4) for satisfactory coincidence of the calculated curves with the experimental temperature dependences of the components of the complex dielectric permittivity.

Introducing frequency decreasing expressions (3, 4), from the physical point of view, can be interpreted as reduction of the concentration of relaxation oscillators in the form of oppositely charged ion pairs involved in dielectric polarization [4]. We consider the process of relaxation polarization in the form of electron hopping between oppositely charged ions of iron located at different distances from each other. In this case, the concentration of oppositely charged ions involved in polarization will largely determine the ε′ values of ferrite permittivity, and the dielectric polarization will depend on the frequency of the electric field and the temperature of the material.

The analysis of the dielectric parameters (table 1) shows that the values of activation energy for each type of the relaxation oscillators are virtually the same for all types of samples, which may indicate similar physical nature of each type of the relaxation oscillators.

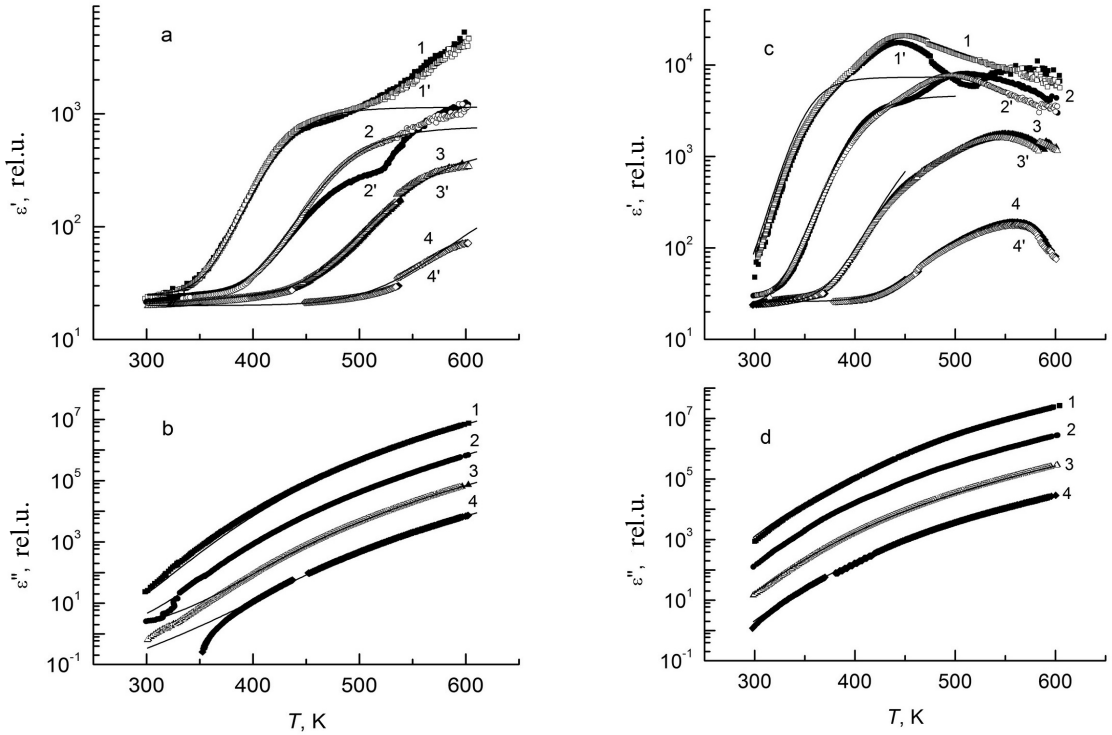


**Figure 1.** Temperature dependence of the real ε′ and imaginary ε″ components of the complex dielectric permittivity under heating (1–4) and cooling (1′–4′) of the ferrite samples, $T_s$= 1283 K, $t_s$ = 4 h (a, b) and $T_s$ = 1373 K, $t_s$ = 4 h (c, d). The frequency of the test signal: 100 Hz (1, 1′), 1 kHz (2, 2′), 10 kHz (3, 3′), 100 kHz (4, 4′).

**Table 1**. Dielectric parameters of lithium-titanium ferrite samples.

| | $T_s$ =1283 (K) | | | $T_s$=1373 (K) | | |
|---|---|---|---|---|---|---|
| | $t_s$ =2 (h) | $t_s$ =4 (h) | $t_s$ =7 (h) | $t_s$ =2 (h) | $t_s$ =4 (h) | $t_s$ =7 (h) |
| q1 | –0.45 | –0.5 | –0.5 | –0.4 | –0.32 | –0.32 |
| q2 | –0.15 | –0.17 | –0.17 | –0.3 | –0.2 | –0.28 |
| B ($c^{q2}$) | 3972 | 3433 | 3287 | 44010 | 26702 | 99560 |
| A ($c^{-q1}$) | $1.48\cdot10^{-6}$ | $2.04\cdot10^{-6}$ | $2\cdot10^{-6}$ | $2.36\cdot10^{-7}$ | $6.4\cdot10^{-8}$ | $3.8\cdot10^{-8}$ |
| $E_{a2}$ (eV) | 0.375 | 0.375 | 0.375 | 0.375 | 0.375 | 0.375 |
| $\varepsilon_\infty$ | 20 | 20 | 20 | 26 | 26 | 26 |
| $\varepsilon_2$ | 25 | 25 | 25 | 23.8 | 23.8 | 23.8 |
| $\tau_{01}$ (s) | $1.2\cdot10^{-7}$ | $1.2\cdot10^{-7}$ | $1.2\cdot10^{-7}$ | $1.2\cdot10^{-7}$ | $1.2\cdot10^{-7}$ | $1.2\cdot10^{-7}$ |
| $E_{a1}$ (eV) | 0.15 | 0.15 | 0.15 | 0.15 | 0.15 | 0.15 |
| $\sigma_{0a}$ $(\Omega\ m)^{-1}$ | $3.18\cdot10^{4}$ | $4.34\cdot10^{4}$ | $3.66\cdot10^{4}$ | $6.66\cdot10^{3}$ | $7.10\cdot10^{3}$ | $5.04\cdot10^{3}$ |
| $E_{a\sigma}$ (eV) | 0.714 | 0.720 | 0.715 | 0.574 | 0.557 | 0.520 |

$E_{a2}$ is the activation energy of the relaxation process for the second type of relaxation oscillators dominant in its concentration; A and B are the frequency-independent parameters in expressions (1) and (2).

However, $E_{a\sigma}$ and $\sigma_{0a}$ values in the ferrite samples sintered at $T_s$=1373 K are considerably higher than those in the samples sintered at $T_s$=1283 K. The electrical conductivity of ceramic materials in the radio frequency region depends on the height of the intergranular potential barrier, which results from the difference between the iron ion concentration in the grain volume and intergranular layer. Redistribution of concentrations of $Fe^{2+}$ and $Fe^{3+}$ ions in these regions relates to diffusion of oxygen ions from the intergranular layer into the grain volume and oxidation of $Fe^{3+}$ ions to $Fe^{2+}$ [2].

To identify unambiguously the electromigration mechanism in the grain volume, we need to measure the conductivity in a higher frequency range of the electric field. In this case, as the frequency increases, the intergranular layer capacitance shunting will cause decrease in the conductivity values. Most of the studies [11] consider the mechanism of electromigration during electron hopping between the localized states in ferrite crystal lattice ions. In this case, electromigration mechanisms and relaxation polarization equivalent, and therefore, the activation energy of electromigration processes at under high frequency electric field should be similar to the energy of relaxation polarization.

In our research, $E_a$ and $E_{a\sigma}$ values are not identical due to the heterogeneous structure of ferrite ceramics and a relatively narrow range of the measuring frequency of the electric field.

The thermogravimetric analysis of the ferrite powder under sintering showed that charges lose their weight under sintering in isothermal curing due to ferrite reduction, i.e. to diffusion of oxygen ions from the material into the atmosphere. Cooling at temperature in the range of T=1273–1073 K results in replacement of the reducing medium with oxidizing atmosphere and mass gain due to the direct oxygen diffusion in the material volume, primarily in the grain boundaries on the powder particle surface. In this case, the effect of sintering time on concentration of $Fe^{2+}$ ions found mostly in the volume of the ferrite grain is not significant since the values of the bulk diffusion coefficient of oxygen ions in the grain are considerably lower if compared to the intergranular layer. The duration of the cooling phase for the sample is limited as well.

The investigation of the sample magnetic characteristics at room temperature showed that the value of saturation magnetization $M_s$ is crucial for samples sintered at $t_s$=2 h and $T_s$=1373 K (table 2). The values correspond to the nominal values of $M_s$ for ferrite 3SCH-18 [5]. As $T_s$ increases, $M_s$ grows, whereas sintering time insignificantly affects the value of $M_s$.

**Table 2**. Values of $M_s$ (G).

| $t_s$ (h) | $T_s$=1283 (K) | $T_s$=1373 (K) |
|---|---|---|
| 2 | 143 | 172 |
| 4 | 156 | 158 |
| 7 | 149 | 165 |

It is known [1, 7] that the values of $M_s$ in the spinel ferrite depend on the distribution of iron cations over sublattices. The more the number of iron cations $Fe^{3+}$ in the octahedral (B) sublattice and the less the number of iron cations in the tetrahedral (A) sublattice, the higher the value of $M_s$.

In this case, the concentration of $Fe^{3+}$ ions in the sublattice B is expected to reach the maximum under sintering at $T_s$=1373 K and $t_s$=2 h.

The values of basic structural parameters for ferrite samples of various types were determined via the diffractometer analysis of ferrite ceramics. The radiograms for each of the samples (powders) obtained with a diffractometer were processed in the program Powder Cell and enabled calculation of the basic structural parameters of ferrite (table 3).

**Table 3**. Structural parameters of ferrite ceramic samples.

| $t_s$ (h) | $T_s$=1283 (K) | | | $T_s$=1373 (K) | | |
|---|---|---|---|---|---|---|
| | content of the main phase (%) | chemical formula | a (Å) | content of the main phase (%) | chemical formula | a (Å) |
| 2 | 92.8 | $Fe_{0.61}Zn_{0.2}Li_{0.19}[Fe_{0.494}Li_{0.229}Ti_{0.25}Mn_{0.025}]O_4$ | 8.365 | 98.9 | $Fe_{0.58}Zn_{0.2}Li_{0.22}[Fe_{0.509}Li_{0.214}Ti_{0.25}Mn_{0.025}]O_4$ | 8.366 |
| 4 | 95.8 | $Fe_{0.57}Zn_{0.2}Li_{0.23}[Fe_{0.514}Li_{0.209}Ti_{0.25}Mn_{0.025}]O_4$ | 8.364 | 89.1 | $Fe_{0.63}Zn_{0.2}Li_{0.17}[Fe_{0.484}Li_{0.239}Ti_{0.25}Mn_{0.025}]O_4$ | 8.367 |
| 7 | 90.9 | $Fe_{0.59}Zn_{0.2}Li_{0.21}[Fe_{0.504}Li_{0.219}Ti_{0.25}Mn_{0.025}]O_4$ | 8.366 | 92.3 | $Fe_{0.63}Zn_{0.2}Li_{0.17}[Fe_{0.484}Li_{0.239}Ti_{0.25}Mn_{0.025}]O_4$ | 8.366 |

Where a is lattice constant.

In this case, the chemical formula for stoichiometric composition of 3SCH-18 ferrite is as follows: $Fe_{0.62}Zn_{0.2}Li_{0.18}[Fe_{0.489}Li_{0.234}Ti_{0.25}Mn_{0.025}]O_4$

As can be seen from the table, the content of the main phase of 3SCH-18 ranges from 89 wt. % to 98 wt. %. Apart from to the main phase, an additional non-magnetic phase of orthoferrite lithium $LiFeO_2$ was found, which "dilutes" the main phase, thereby affects the magnetization value, namely, it reduces magnetization.

The values of lattice constant (a) appeared to be close for all ferrite samples regardless of the changes expected during redistribution of iron cations in the sublattices as the radius of $Fe^{2+}$ ions is greater than that of $Fe^{3+}$ ions.

Table 3 also shows that redistribution of iron ions in the sublattices of the samples with different sintering parameters indicates a pattern when the sintering time with the greatest values of $M_s$ corresponds to each value of $T_s$ with the highest concentration of iron ions $Fe^{3+}$ in the sublattice B.

If the mechanism of electrical conductivity and relaxation polarization of ferrite is considered in terms of the model of hopping over localized states between $Fe^{2+}$ and $Fe^{3+}$ ions located in the octahedral (B) sublattice [8, 9, 11], the concentration of relaxation oscillators and therefore $\varepsilon'$ values will depend on the cationic distribution of iron ions. Thus, the transfer of iron ions into octahedral positions under varying modes of ferrite ceramics sintering will lead to an increase in $\varepsilon'$ values. The comparison of the experimental data illustrates the tendency to this dependence (tables 1 and 3).

## 4. Conclusion

The comparative analysis of the data obtained through the diffraction analysis of powder samples (Table 3) and experimental data showed that $M_s$ values correlate with the values of $Fe^{3+}$ ion concentration in the octahedral (B) sublattice of the ferrite spinel and the concentration of the 3SCH-18 main phase for samples sintered both at $T_s$=1283 K and $T_s$=1373 K.

The obtained results can be used to choose a technological mode for lithium-titanium ferrite ceramics sintering in order to obtain an optimal set of operating parameters for ferrite products.

## 5. Acknowledgements

The research was supported by the Ministry of Education and Science of the Russian Federation in part of the “Science” program.

## References

[1] Gorter E V 1955 *Uspehi Fiz. Nauk [in Russian]* **10** 279–346
[2] Surzhikov A P, Pritulov A M, Peshev V V and Malyshev A V et al 2001 *Russ. Phys. J.* **44** 11 1244–47
[3] Malyshev A V and Peshev V V 2007 *Russ. Phys. J.* **50** 2 161-164
[4] Surzhikov A P, Lysenko E N and Malyshev A V et al 2014 *Russ. Phys. J.* **57** 5 621–626
[5] Malyshev A V, Lysenko E N and Vlasov V A 2015 *Ceramics International* **41** 10 13671–75
[6] Smit J and Wijn H P J 1959 Ferrites. Physical properties of ferrimagnetic oxides in relation to their technical applications (Philips Technical Library: Eindhoven) p 299
[7] Krupichka S Physics of ferrites and related magnetic oxides 1976 [in Russian] (Moscow: Nauka) p 683
[8] Koops C G 1951 *Phys. Rev.* V **33** 1 121–124
[9] Watawe S C et al 2000 *J. of Magn. and Magn. Mat.* **214** 55–60
[10] Kreslin V Yu and Naiden E P 2002 *Pribory i tehnika experimenta [in Russian]* 1 63–66
[11] Lipare A Y et al 2003 *Materials Chemistry and Physics* **81** 108–115